

## SPECIAL ISSUE "NANO-POLYCRYSTALLINE DIAMOND AND ITS APPLICATIONS"

### Recent progress in high-pressure X-ray absorption spectroscopy studies at the ODE beamline

Lucie Nataf<sup>a</sup>, François Baudelet<sup>a</sup>, Alain Polian<sup>a</sup>, Inga Jonane<sup>b</sup>, Andris Anspoks<sup>b</sup>, Alexei Kuzmin<sup>b</sup> and Tetsuo Irifune<sup>c</sup>

<sup>a</sup>Synchrotron SOLEIL, l'Orme des Merisiers, Saint-Aubin, Gif-sur-Yvette, France; <sup>b</sup>Institute of Solid State Physics, University of Latvia, Riga, Latvia; <sup>c</sup>Geodynamics Research Center, Ehime University, Matsuyama, Ehime, Japan

#### ARTICLE HISTORY

Compiled February 25, 2020

#### ABSTRACT

High-pressure energy-dispersive X-ray absorption spectroscopy is a valuable structural technique, especially, when combined with a nano-polycrystalline diamond anvil cell. Here we present recent results obtained using the dispersive setup of the ODE beamline at SOLEIL synchrotron. The effect of pressure and temperature on the X-ray induced photoreduction is discussed on the example of nanocrystalline CuO. The possibility to follow local environment changes during pressure-induced phase transitions is demonstrated for  $\alpha$ -MoO<sub>3</sub> based on the reverse Monte Carlo simulations.

#### KEYWORDS

High-pressure; nano-polycrystalline diamond anvil cell; XANES; EXAFS

### 1. Introduction

An alternative to the traditional pattern of beamlines dedicated to the X-ray absorption spectroscopy, based on a two-crystal scanning mode, is given by the use of dispersive optics [1–4]. In this technique, a bent crystal is used as a monochromator, and the setup is usually called Energy Dispersive EXAFS (EDE). The continuous change of the Bragg incidence along the bent crystal opens an energy range in the reflected beam. The correlation between position and energy of the X-ray is exploited thanks to a position sensitive detector. The setup can be used to acquire both the X-ray absorption near edge structure (XANES) as well as extended X-ray absorption fine structure (EXAFS).

The EDE beamline at SOLEIL synchrotron, called ODE for Optic Dispersive EXAFS [5], has extensively developed high-pressure XAS (X-ray Absorption Spectroscopy) and XMCD (X-ray Magnetic Circular Dichroism) techniques. The XMCD

---

CONTACT François Baudelet. Email: francois.baudelet@synchrotron-soleil.fr Address: Synchrotron SOLEIL, l'Orme des Merisiers, Saint-Aubin, BP 48, 91192 Gif-sur-Yvette, France

Alexei Kuzmin. Email: a.kuzmin@cfi.lu.lv Address: Institute of Solid State Physics, University of Latvia, Kengaraga street 8, LV-1063 Riga, Latvia

activity was already presented in [6]. Here we report on some high-pressure measurements done with a nano-polycrystalline diamond anvil cell (NDAC) [7].

The main advantages of dispersive XAS are the focusing optics, the short acquisition time, and the great stability during the measurements due to the absence of any mechanical movement. This advantage allows the study of small samples, mandatory in the case of high-pressure studies, where the sample chamber is a hole in a gasket sandwiched between two diamonds. The EDE technique is particularly adapted for deglitching due to its live measuring process with classical diamonds, however, there are some limits in the 10 keV range. The use of NDAC allows one to improve significantly the quality of the experimental signal eliminating spurious contributions from the diamond Bragg reflections [8]. This opens the route of many new possibilities as seen in the following contributions of XAS pressure measurements.

## 2. X-ray absorption spectroscopy at high-pressure

### 2.1. XANES as a probe of X-ray photoreduction

High-intensity X-ray beams at modern sources of synchrotron radiation can cause radiation damage to a material. The effect is well known in the case of metal-organic complexes [9–11]. This problem may be of particular importance for beamlines with the energy-dispersive setup when a polychromatic X-ray beam with the spectral range of several hundred electron-volts is focused to the spot of several tens of microns on the sample located in the diamond anvil cell. In particular, when high-pressure measurements are performed, the indirect damage of the sample placed in a solution, which plays the role of the pressure-transmitting medium, can occur due to the radiolysis of the latter. In the radiolysis process, reducing radicals such as solvated electrons and hydrogen atoms are produced upon X-ray irradiation of the solution and are responsible for the sample change [12,13]. For example, the radiolysis can lead to a reduction of metal ions in aqueous solutions and is used for synthesis of metal nanoparticles [14–16].

Recently, we have demonstrated X-ray induced photoreduction of nanocrystalline CuO, and its dependence on crystallite size, temperature and pressure [17]. Nanocrystalline CuO (nano-CuO) powder samples with the average crystallite size of 8 nm and 20 nm were prepared by a decomposition of Cu(OH)<sub>2</sub> precipitate in air at 130 °C and 150 °C, respectively. The Cu K-edge XANES spectra were collected in the pressure range of 0-23 GPa and the temperature range of 10-300 K. The sample pressure and temperature were controlled using a membrane-type nano-polycrystalline diamond anvil cell (NDAC) [7,8] and liquid helium cryostat. The use of NDAC allowed us to accumulate the experimental data free from Bragg peaks due to the diamonds. The polychromatic photon flux on the sample was about 10<sup>9</sup> photons/s/eV in 25×35 μm FWHM.

The sensitivity of the Cu K-edge XANES in nano-CuO (8 nm) to temperature and pressure is shown in Fig. 1(a). The emergence of metallic copper is visible at  $T=260$  K and  $P=2$  GPa after 70 minutes of exposure to X-rays as an increasing shoulder at 8983 eV and a decreasing main peak at 9000 eV. X-ray induced photoreduction occurs more rapidly at higher temperatures and lower pressure. For larger crystallite size (20 nm), the reduction process takes longer time (Fig. 1(b)). At  $T=300$  K and  $P=0.2$  GPa, copper oxide is fully converted into metallic copper after about 90 minutes of irradiation. However, an increase of pressure to 23 GPa stabilizes the oxide phase.

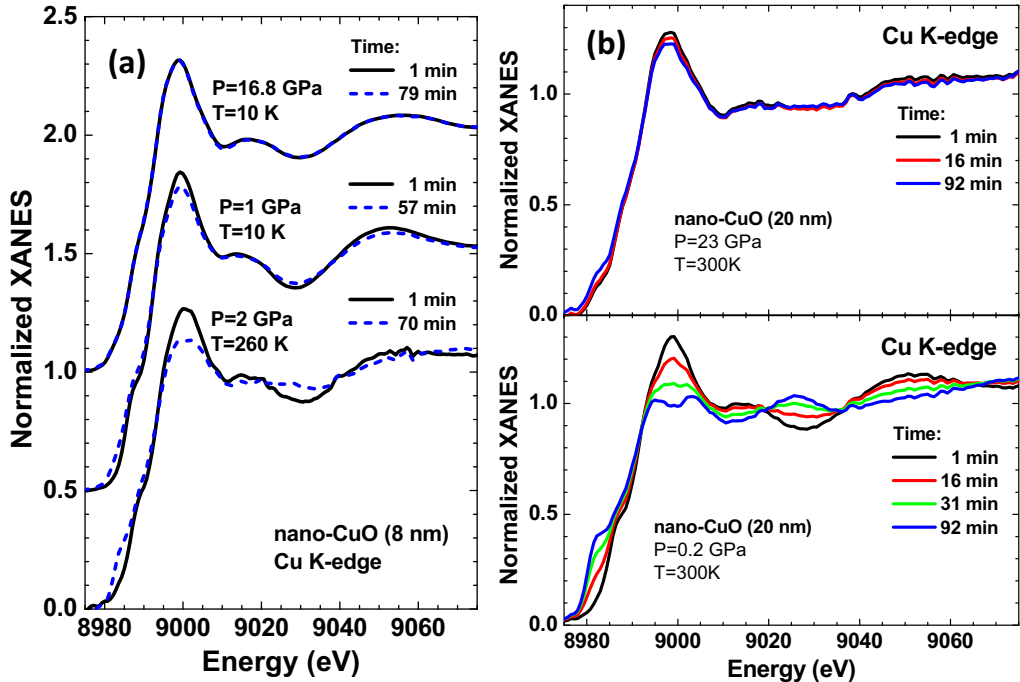


**Figure 1.** (a) Temperature, pressure and time dependence of the Cu K-edge XANES of nano-CuO (8 nm). Solid line – starting spectrum, dashed line – spectrum after long time (57-79 min) exposition. Spectra are shifted vertically for clarity. (b) Pressure and time dependence of the Cu K-edge XANES of nano-CuO (20 nm). Upper panel – P=23 GPa, lower panel – P=0.2 GPa.

Note that the photoreduction was not observed for microcrystalline CuO at similar conditions. Thus, the rate of nano-CuO photoreduction to metallic copper increases with decreasing nanoparticle size but can be reduced by a decrease of temperature or an increase of pressure. Performing experiment at low temperatures decreases the mobility of reducing radicals [18,19], whereas an increase of pressure results in CuO nanoparticles agglomeration thus restricting their free surface and impeding reduction. The obtained results suggest that possible radiation damage should be taken into account in experiments with high-flux X-ray beams, especially, in the case of nanosized materials.

## 2.2. Pressure-induced phase transitions probed by EXAFS

The sensitivity of EXAFS to the local atomic structure of a material and recent developments in the EXAFS data analysis based on the reverse Monte Carlo (RMC) simulations [20] provide an invaluable tool to follow pressure-induced phase transitions. However, high-quality experimental data remain the main limiting factor to unleash the potential of the method.

The pressure-induced (up to 36 GPa) transformations in 2D layered oxide  $\alpha$ -MoO<sub>3</sub> were studied at the Mo K-edge in [21]. Good quality experimental EXAFS data were acquired using the NDAC cell and allowed us to perform analysis up to 6 Å using the RMC method. The structural models obtained by RMC give the Mo K-edge EXAFS spectra in good agreement with the experimental ones (Fig. 2). The corresponding atomic coordinates were used to calculate the radial distribution functions  $g(R)$  for

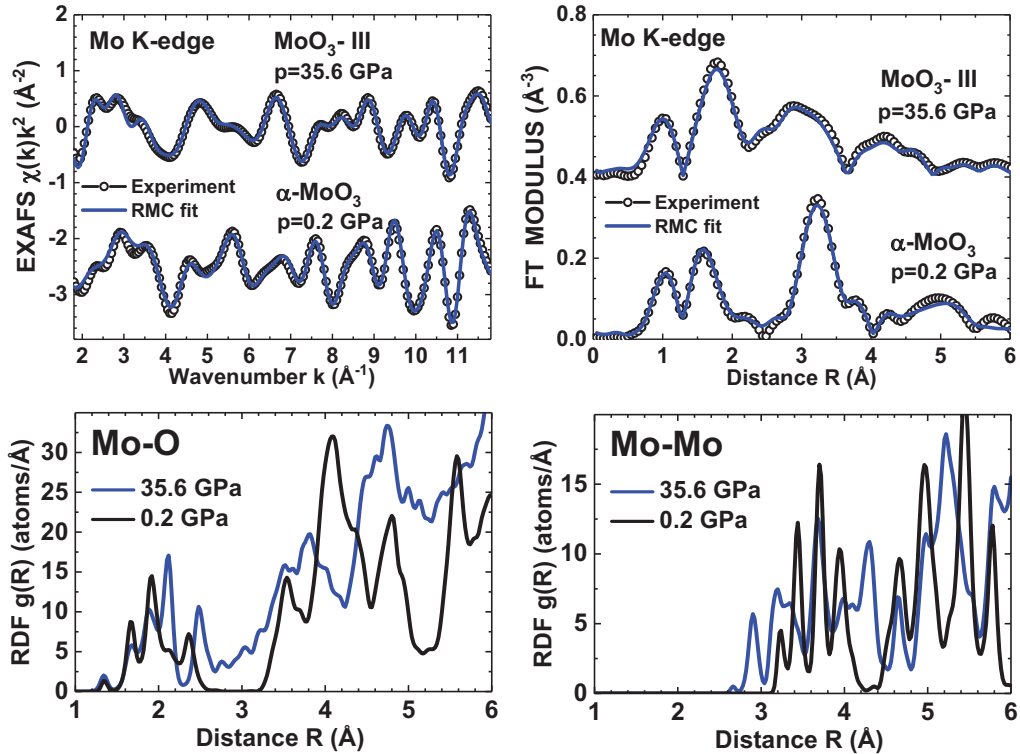


**Figure 2.** Results of the RMC-EXAFS calculations for  $\alpha$ - $\text{MoO}_3$  (0.2 GPa) and  $\text{MoO}_3$ -III (35.6 GPa) phases. Upper row: comparison of the experimental and calculated Mo K-edge EXAFS spectra  $\chi(k)k^2$  and their Fourier transforms. Curves are shifted vertically for clarity. Lower row: the radial distribution functions (RDFs) for Mo–O and Mo–Mo atom pairs reconstructed by the RMC method.

Mo–O and Mo–Mo atom pairs as a function of pressure and allowed us to follow the details of local structure transformations upon phase transitions (Fig. 2).

At room temperature, molybdenum trioxide exhibits two phase transitions upon compression in the range of 0–43 GPa [22].  $\alpha$ - $\text{MoO}_3$  transforms to monoclinic  $\text{MoO}_3$ -II phase ( $P2_1/m$ ) at  $\sim 12$  GPa, and, next, to monoclinic  $\text{MoO}_3$ -III phase ( $P2_1/c$ ) at  $\sim 25$  GPa. The first two phases ( $\alpha$ - $\text{MoO}_3$  and  $\text{MoO}_3$ -II) have layered structure composed of strongly distorted  $\text{MoO}_6$  octahedra, whereas a collapse of the interlayer gap occurs in  $\text{MoO}_3$ -III phase [22].

The difference between  $\alpha$ - $\text{MoO}_3$  and  $\text{MoO}_3$ -III phases is well established by EXAFS. The transition is accompanied by a change of the Mo–O–Mo angles between neighbouring molybdenum-oxygen octahedra from  $\sim 142^\circ$  and  $\sim 168^\circ$  in  $\alpha$ - $\text{MoO}_3$  [23] to  $\sim 149^\circ$  in  $\text{MoO}_3$ -III [22]. The disappearance of the Mo–O–Mo angle equal to  $168^\circ$  is responsible for a decrease of the second shell peak (at  $\sim 3.2$  Å in Fig. 2) amplitude in the Fourier transform of the EXAFS spectrum of  $\text{MoO}_3$ -III due to a reduction of the multiple-scattering (MS) effects within the Mo–O–Mo atomic chains.

The reconstruction of the local environment around molybdenum using the reverse Monte Carlo (RMC) method [20] shed light on the pressure dependence of the radial distribution functions (RDFs) for Mo–O and Mo–Mo atom pairs in details.

At small pressure of about 0.2 GPa, there are three groups of two oxygen atoms each located at  $\sim 1.70$ ,  $1.96$  and  $2.26$  Å, which form strongly distorted  $\text{MoO}_6$  octahedra in  $\alpha$ - $\text{MoO}_3$ . At high pressure (35.6 GPa), the collapse of layered structure leads to an increase of molybdenum coordination. Six nearest oxygen atoms from the same layer

are responsible for the peaks at  $\sim 1.68$ ,  $1.88$  and  $2.12$  Å, whereas the 7th oxygen atom bridging two layers is located at  $\sim 2.48$  Å. The high pressure influences also the Mo–Mo distribution, leading to a shortening of the distance between neighboring molybdenum-oxygen polyhedra connected by edges (peaks at  $2.9$  and  $3.25$  Å). Thus, the change of the molybdenum local environment upon phase transitions is well evidenced by the RMC analysis of high-pressure Mo K-edge EXAFS spectra.

### 3. Conclusion

In this paper, we describe the potential of high-pressure energy-dispersive X-ray absorption spectroscopy (XANES/EXAFS) in combination with a nano-polycrystalline diamond anvil cell. The experimental setup is well suited for such measurements, making it possible to obtain experimental data of good quality, being free from the Bragg contribution from diamonds. At the same time, the accessible spectral range of the dispersive setup is restricted by the linear size of the detector, which imposes limitations on the resolution in real space. In addition, high intensity of X-rays focused on a sample can cause radiation damage.

Two examples of high-pressure XAS studies of transition metal oxide compounds (CuO and MoO<sub>3</sub>) are discussed. They illustrate the sensitivity of copper oxide nanoparticles to reduction under X-ray irradiation and the ability to track local structural changes during phase transition in a 2D layered-type molybdenum trioxide using an advanced analysis method based on the reverse Monte Carlo algorithm.

### Disclosure statement

No potential conflict of interest was reported by the authors.

### Funding

A.K. and I.J. are grateful to the Latvian Council of Science project no. lzp-2018/2-0353 for financial support. The research leading to these results has been partially supported by the project CALIPSOplus under the Grant Agreement No. 730872 from the EU Framework Programme for Research and Innovation HORIZON 2020.

### References

- [1] Fontaine A, Baudelet F, Dartyge E, et al. Two time-dependent, focus-dependent experiments using the energy-dispersive spectrometer at LURE. *Rev Sci Instrum.* 1992; 63:960–965.
- [2] Blank H, Neff B, Steil S, et al. A new energy dispersive x-ray monochromator for soft x-ray applications. *Rev Sci Instrum.* 1992;63:1334–1337.
- [3] D’Acapito F, Boscherini F, Marcelli A, et al. Dispersive EXAFS apparatus at Frascati. *Rev Sci Instrum.* 1992;63:899–901.
- [4] Dent AJ, Wells MP, Farrow RC, et al. Combined energy dispersive EXAFS and x-ray diffraction. *Rev Sci Instrum.* 1992;63:903–906.
- [5] Baudelet F, Kong Q, Nataf L, et al. ODE: a new beam line for high-pressure XAS and XMCD studies at SOLEIL. *High Pressure Res.* 2011;31:136–139.

- [6] Baudelet F, Nataf L, Torchio R. New scientific opportunities for high pressure research by energy-dispersive XMCD. *High Pressure Res.* 2016;36:429–444.
- [7] Tetsuo I, Ayako K, Shizue S, et al. Materials: ultrahard polycrystalline diamond from graphite. *Nature.* 2003;421:599–600.
- [8] Ishimatsu N, Matsumoto K, Maruyama H, et al. Glitch-free x-ray absorption spectrum under high pressure obtained using nano-polycrystalline diamond anvils. *J Synchrotron Rad.* 2012;19:768–772.
- [9] Oliéric V, Ennifar E, Meents A, et al. Using X-ray absorption spectra to monitor specific radiation damage to anomalously scattering atoms in macromolecular crystallography. *Acta Crystallogr D.* 2007;63:759–768.
- [10] Holton JM. A beginner’s guide to radiation damage. *J Synchrotron Rad.* 2009;16:133–142.
- [11] Kubin M, Kern J, Guo M, et al. X-ray-induced sample damage at the Mn L-edge: a case study for soft X-ray spectroscopy of transition metal complexes in solution. *Phys Chem Chem Phys.* 2018;20:16817–16827.
- [12] Jonah CD. A short history of the radiation chemistry of water. *Radiat Res.* 1995;144:141–147.
- [13] Le Caer S. Water radiolysis: influence of oxide surfaces on H<sub>2</sub> production under ionizing radiation. *Water.* 2011;3:235–253.
- [14] Joshi S, Patil S, Iyer V, et al. Radiation induced synthesis and characterization of copper nanoparticles. *Nanostruct Mater.* 1998;10:1135–1144.
- [15] Lee HJ, Je JH, Hwu Y, et al. Synchrotron X-ray induced solution precipitation of nanoparticles. *Nucl Instrum Methods B.* 2003;199:342–347.
- [16] Oyanagi H, Orimoto Y, Hayakawa K, et al. Nanoclusters synthesized by synchrotron radiolysis in concert with wet chemistry. *Sci Rep.* 2014;4:7199.
- [17] Kuzmin A, Anspoks A, Nataf L, et al. Influence of pressure and temperature on X-ray induced photoreduction of nanocrystalline CuO. *Latvian J Phys Tech Sci.* 2018;55:13–19.
- [18] Corbett MC, Latimer MJ, Poulos TL, et al. Photoreduction of the active site of the metalloprotein putidaredoxin by synchrotron radiation. *Acta Crystallogr D.* 2007;63:951–960.
- [19] Meents A, Gutmann S, Wagner A, et al. Origin and temperature dependence of radiation damage in biological samples at cryogenic temperatures. *Proc Natl Acad Sci USA.* 2010; 107:1094–1099.
- [20] Timoshenko J, Kuzmin A, Purans J. EXAFS study of hydrogen intercalation into ReO<sub>3</sub> using the evolutionary algorithm. *J Phys: Condens Matter.* 2014;26:055401.
- [21] Jonane I, Anspoks A, Nataf L, et al. Pressure-induced structural changes in  $\alpha$ -MoO<sub>3</sub> probed by X-ray absorption spectroscopy. *IOP Conf Series: Mater Sci Eng.* 2019; 503:012018.
- [22] Liu D, Lei W, Hao J, et al. High-pressure Raman scattering and x-ray diffraction of phase transitions in MoO<sub>3</sub>. *J Appl Phys.* 2009;105:023513.
- [23] Åsbrink S, Kihlberg L, Malinowski M. High-pressure single-crystal X-ray diffraction studies of MoO<sub>3</sub>. I. Lattice parameters up to 7.4 GPa. *J Appl Crystallogr.* 1988;21:960–962.